

See discussions, stats, and author profiles for this publication at: <https://www.researchgate.net/publication/231272277>

# Effective and Low-Cost Platinum Electrodes for Microbial Fuel Cells Deposited by Electron Beam Evaporation

ARTICLE *in* ENERGY & FUELS · AUGUST 2007

Impact Factor: 2.79 · DOI: 10.1021/ef070160x

---

CITATIONS

23

---

READS

47

7 AUTHORS, INCLUDING:



David Perello

Sungkyunkwan University

33 PUBLICATIONS 343 CITATIONS

SEE PROFILE



Sung Kwon Cho

University of Pittsburgh

61 PUBLICATIONS 2,299 CITATIONS

SEE PROFILE

# Effective and Low-Cost Platinum Electrodes for Microbial Fuel Cells Deposited by Electron Beam Evaporation

Ho Il Park,<sup>†</sup> Usman Mushtaq,<sup>†</sup> David Perello,<sup>†</sup> Innam Lee,<sup>†</sup> Sung Kwon Cho,<sup>‡</sup>  
Alexander Star,<sup>§</sup> and Minhee Yun<sup>\*,†</sup>

Department of Electrical and Computer Engineering, University of Pittsburgh, Pittsburgh, Pennsylvania,  
Department of Mechanical Engineering and Materials Science, University of Pittsburgh, Pittsburgh,  
Pennsylvania, and Department of Chemistry, University of Pittsburgh, Pittsburgh, Pennsylvania

Received March 28, 2007. Revised Manuscript Received June 7, 2007

A microbial fuel cell (MFC) is a device that converts chemical energy to electrical energy through the catalytic reaction of microorganisms. In this paper, electricity generation was investigated in microbial fuel cells using e-beam deposited Pt electrodes to improve efficiency and minimize Pt loading. We deposited Pt on carbon paper electrodes using an e-beam evaporator and imaged microscopic structures of the Pt deposited electrodes using scanning electron microscopy and atomic force microscopy. Although the e-beam electrode had the least thick Pt layer (1000 Å) among many tested electrode types (Pt-black = 1500 Å and commercial electrode = 2500 Å), it showed excellent coverage and Pt uniformity, resulting in minimal loading of Pt. In MFC testing, the e-beam Pt electrode installed only on the anode (carbon paper electrode on the cathode) produced the highest peak value of 0.42 A/m<sup>2</sup> in the current density, which was about 2 times higher than when the Pt-black anode electrode or E-Tek commercial Pt anode electrode was used. After 45 h of microbial fuel cell running with the Pt electrode on the anode, the carbon electrode on the cathode was also replaced with an e-beam electrode. This replacement generated an immediate rise in current density, reaching a second peak of 0.50 A/m<sup>2</sup>. Considering the mass-specific current density, which represents the current density per unit Pt thickness, the e-beam electrode was the most effective with minimal Pt loading. The mass-specific current density for the e-beam electrodes was 2.5 times higher than that for the E-Tek commercial electrodes. These promising results suggest the high potential of e-beam-deposited Pt electrodes in improving microbial fuel cell efficiency with minimal Pt loading.

## Introduction

A microbial fuel cell (MFC) is a device that converts chemical energy to electrical energy through the catalytic reaction of microorganisms.<sup>1</sup> Typical MFCs mainly consist of anode and cathode compartments separated by a cation-specific membrane.<sup>2</sup> Fuel typically for which wastewater or food processing wastewater is used is oxidized by microorganisms that produce electrons and protons in the anode compartment.<sup>3</sup> The electrons flow via a wire to the cathode compartment while the protons pass through the separating membrane, eventually reaching the cathode compartment. Both electrons and protons are eventually consumed in the cathode compartment, reducing oxygen to form water.<sup>4,5</sup> In this process, electric power can be extracted by applying electric loads to the wire.

Currently, MFCs seem to promise an alternative energy source. As nonrenewable energy sources such as coal and

petroleum become limited, the use of renewable sources such as wastewater and food processing wastewater becomes more demanding. This is one of the main reasons to draw more attention to MFCs. Of equal importance, after the oxidation/reduction reactions in MFCs, the used wastewater or food processing wastewater becomes more sanitary and thus environmentally friendly. Therefore, MFCs can be used even in space cabins and habitats to purify astronauts' excretions and possibly recycle them into clean water,<sup>6</sup> as well as to generate energy.

However, MFCs typically have shown lower levels of efficiency in power generation compared to other types of fuel cells,<sup>7</sup> which has critically restricted their practical use for an energy source. To improve their efficiency, numerous approaches have been made. Some groups have modified electrode materials using metal, surfactants, and organic materials.<sup>8–10</sup>

\* Corresponding author. Phone: (412) 648-8989. Fax: (412) 648-8003. E-mail: yunmh@engr.pitt.edu.

<sup>†</sup> Department of Electrical and Computer Engineering.

<sup>‡</sup> Department of Mechanical Engineering and Materials Science.

<sup>§</sup> Department of Chemistry.

(1) Akiba, T.; Bennetto, H. P.; Stirling, J. L.; Tanaka, K. Electricity generation from alkalotrophic organisms. *Biotechnol. Lett.* **1985**, *9*, 611–616.

(2) Gil, G. C.; Chang, I. S.; Kim, B. H.; Kim, M.; Jang, J. K.; Park, H. S.; Kim, H. J. Operational parameters affecting the performance of a mediator-less microbial fuel cell. *Biosens. Bioelectron.* **2003**, *18*, 327–334.

(3) Oh, S.; Logan, B. E. Hydrogen and electricity production from a food processing wastewater using fermentation and microbial fuel cell technologies. *Water Res.* **2005**, *39*, 4673–4682.

(4) Allen, R. M.; Bennetto, H. P. Microbial fuel cell. *Appl. Biochem. Biotechnol.* **1993**, *39/40*, 24–40.

(5) Chang, I. S.; Moon, H.; Bretschger, O.; Jang, J. K.; Park, H. I.; Neelson, K. H.; Kim, B. H. Electrochemically active bacteria (EAB) and mediator-less microbial fuel cells. *J. Microbiol. Biotechnol.* **2006**, *16*, 163–177.

(6) Lovley, D. R. Microbial energizers: Fuel cells that keep on going. Microbes that produce electricity by oxidizing organic compounds in biomass may someday power useful electronic devices. *Microbes* **2006**, *1*, 323–329.

(7) Cheng, S.; Liu, H.; Logan, B. E. Power densities using different cathode catalysts (Pt and CoTMP) and polymer binder (Nafion and PTFE) in single chamber microbial fuel cells. *Environ. Sci. Technol.* **2006**, *40*, 364–369.

(8) Chen, P.; Fryling, M. A.; McCreery, R. L. Electron transfer kinetics at modified carbon electrode surface: The role of specific surface sites. *Anal. Chem.* **1995**, *67*, 3115–3122.

(9) DuVall, S. H.; McCreery, R. L. Control of catechol and hydroquinone electron-transfer kinetics on native and modified glassy carbon electrodes. *Anal. Chem.* **1999**, *71*, 4594–4602.

Other groups have used different mediators such as thionine,<sup>11</sup> viologens,<sup>1</sup> and methylene blue.<sup>12</sup> Recently, ferricyanide<sup>13,14</sup> and peroxide<sup>15</sup> have been used to increase the rate of the oxygen reduction reaction. More recently, membraneless MFCs<sup>15,16</sup> have been devised, and a biofilm has been employed on cathode electrodes.<sup>18</sup> Even though the above approaches have made improvements to some degree, it is known that the most attractive and effective is to employ Pt as an electrocatalyst on the electrodes. Pt, a noble metal, is known as one of the most widely used and efficient electrocatalysts for fuel cells.<sup>19,20</sup> It is often utilized in Pt-metal alloy forms such as Pt/Ni,<sup>21</sup> Pt/Cr,<sup>22</sup> and Pt/Ru<sup>23,24</sup> or combined with other binders such as polyaniline,<sup>25</sup> nafion,<sup>26</sup> poly tetrafluoroethylene (PTFE)<sup>7</sup> and cobalt tetramethylphenyl-porphyrin (CoTMPP).<sup>7</sup>

The use of Pt as an electrocatalyst results in one major drawback. Pt is extremely expensive, causing significant cost problems in fuel cell manufacturing and production.<sup>20</sup> Therefore, recent research activities have been focused on minimizing the loading amount of Pt<sup>27</sup> as well as other precious metals,<sup>20</sup> and on enhancing their catalytic activities. In H<sub>2</sub>/air-fed polymer electrolyte membrane fuel cells,<sup>27</sup> highly dispersed Pt-black and Pt nanoparticles have been grown on carbon (Pt/C) in the membrane/electrode assembly using an electrochemical deposi-

tion method. This has resulted in a reduction of Pt loading down to 3000~4000 Å in thickness. Similarly, another study<sup>28</sup> used Pt layers of 250~2000 Å. In addition, various electrode configurations with electrochemically deposited Pt layers were implemented in relation to microbial fuel cells: for example, 1750~2500 Å Pt on electrodes (Mahlon et al.<sup>29</sup>), 2500 Å Pt on electrodes in a nafion solution (Liu et al.<sup>10</sup>), 1400 Å Pt on graphite electrodes in a nafion solution (Pham et al.<sup>26</sup>), 1750 and 2500 Å Pt by way of using Pt/Ru of 1:1 molar ratio (Logan et al.<sup>17</sup>), and 500 ~ 10 000 Å Pt with PTFE or CoTMPP (Cheng et al.<sup>7</sup>). These configurations were often incorporated with physical dispersity generated by air spray guns. Among the aforementioned cases, Cheng et al.<sup>7</sup> reported the lowest Pt loading on cathode electrodes (500 Å). In this case, however, the thin Pt layers suffered from nonuniformity and poor activity.<sup>7,30</sup>

To obviate these problems, more controllable deposition methods with better uniformity are highly desired. An e-beam evaporation deposition method, which is commonly used in micro- and nanofabrication, is known to produce reproducible and reliable thin layers of Pt as well as other materials whose thicknesses range from tens of angstroms to thousands of micrometers. Furthermore, this method is highly controllable and cost-effective, providing improved structural properties in deposited layers.<sup>31</sup>

In this paper, we apply the e-beam evaporation method to deposit Pt nano layers uniformly on microbial fuel cell electrodes, to apply the e-beam-deposited Pt electrodes to a microbial fuel cell, and to examine their performance in terms of current density and power generation. Finally, the test results of the e-beam electrodes are compared with those of electrochemically deposited Pt electrodes, commercial Pt electrodes, and carbon paper electrodes.

## Preparation of the Experiment

**Anaerobic Sludge.** Anaerobic sludge was collected from the wastewater treatment plant of the Franklin Township Municipal Sanitation Authority in Pittsburgh. The anaerobic sludge was inoculated using artificial wastewater, which contained 50 mM of phosphate buffer (pH 7.0), glucose and glutamate,<sup>32</sup> trace mineral solution,<sup>33</sup> and salt solution.<sup>2</sup>

**Electrode Preparation.** Plain Toray carbon paper (TGPH-120, E-Tek, U.S.A.) was used as the electrode substrate in this study. Pt depositions on the electrodes were accomplished via two different methods: (1) Pt of 1500 Å thickness was deposited on the carbon paper electrodes using electrochemical deposition (Pt-black). The potential cycling between 0.5 and -2.0 V at a rate of 500 mV/s was applied to the carbon paper electrodes, which were immersed

(10) Liu, H.; Ramnarayanan, R.; Logan, B. E. Electricity generation using an air-cathode single chamber microbial fuel cell in the presence and absence of a proton exchange membrane. *Environ. Sci. Technol.* **2004**, *38*, 4040–4046.

(11) Bennetto, H. P.; Delaney, G. M.; Mason, J. R.; Roller, H. D.; Stirling, J. L.; Thurston, D. F. The source of fuel cell: Efficient biomass conversion using a microbial catalyst. *Biotechnol. Lett.* **1985**, *7*, 699–704.

(12) Roller, H. D.; Bennetto, H. P.; Delaney, G. M.; Mason, J. R.; Stirling, J. L.; Thurston, D. F. Electron-transfer coupling in microbial fuel cells: 1. Comparison of redox-mediator reduction rates and respiratory rates of bacteria. *J. Chem. Technol. Biotechnol.* **1984**, *34B*, 3–12.

(13) Bond, D. R.; Lovley, D. R. Electricity production by *Geobacter sulfurreducens* attached to electrodes. *Appl. Environ. Microbiol.* **2003**, *64*, 3102–3105.

(14) Rabaey, K.; Lissens, G.; Siciliano, S. D.; Verstraete, W. A microbial fuel cell capable of converting glucose to electricity at high rate and efficiency. *Biotechnol. Lett.* **2003**, *25*, 1531–1535.

(15) Tartakovsky, B.; Guiot, S. R. A comparison of air and hydrogen peroxide oxygenated microbial fuel cell reactors. *Biotechnol. Prog.* **2006**, *22*, 241–246.

(16) Jang, J. K.; Pham, T. H.; Chang, I. S.; Kang, K. H.; Moon, H.; Cho, K. S.; Kim, H. B. Construction and operation of a novel mediator- and membrane-less microbial fuel cell. *Process Biochem. (Oxford, U.K.)* **2004**, *39*, 1007–1012.

(17) Logan, B. E.; Murano, C.; Scott, K.; Gray, N. D.; Head, I. M. Electricity generation from cysteine in a microbial fuel cell. *Water Res.* **2005**, *39*, 942–952.

(18) Allison, R.; Haluk, B.; Zbigniew, L. Microbial fuel cell using anaerobic respiration as an anodic reaction and biomineralized manganese as a cathodic reactant. *Environ. Sci. Technol.* **2005**, *39*, 4666–4671.

(19) Mehta, V.; Cooper, J. S. Review and analysis of PEM fuel cell design and manufacturing. *J. Power Source* **2003**, *1443*, 32–40.

(20) Lin, R. B.; Shin, S. M. Kinetic analysis of the hydrogen oxidation reaction on Pt-black/Nafion electrode. *J. Solid State Electrochem.* **2006**, *10*, 243–249.

(21) Paulus, U. A.; Wokaun, A.; Scherer, G. G. Oxygen reduction on carbon-supported Pt-Ni and Pt-Co alloy catalysts. *J. Phys. Chem. B* **2002**, *106*, 4181–4191.

(22) Min, M.; Cho, J.; Cho, K.; Kim, H. Particle size and alloying effects of Pt-based alloy catalysts for fuel cell applications. *Electrochim. Acta* **2000**, *45*, 4211–4217.

(23) Hoster, H.; Iwasita, T.; Baumgärtner, H.; Vielstich, W. Pt-Ru model catalysts for anodic methanol oxidation: Influence of structure and composition on the reactivity. *Phys. Chem. Chem. Phys.* **2001**, *3*, 337–346.

(24) Brankovic, S. R.; Wang, J. X.; Adžić, R. R. Submonolayers on Ru nanoparticles a novel low Pt loading, High Co tolerance fuel cell electrocatalyst. *Electrochem. Solid-State Lett.* **2001**, *4*, A217–A220.

(25) Schröder, U.; Niessen, J.; Scholz, F. A generation of microbial fuel cells with current output boosted by more than one order of magnitude. *Angew. Chem., Int. Ed. Engl.* **2003**, *32*, 2880–2883.

(26) Pham, T. H.; Jang, J. K.; Chang, I. S.; Kim, B. H. Improvement of cathode reaction of a mediatorless microbial fuel cell. *J. Microbiol. Biotechnol.* **2004**, *12*, 324–329.

(27) Gasteiger, H. A.; Kocha, S. S.; Sompalli, B.; Wagner, F. T. Activity benchmarks and requirements for Pt, Pt-alloy, and non-Pt oxygen reduction catalysts for PEMFCs. *Appl. Catal., B* **2005**, *56*, 9–35.

(28) Gasteiger, H. A.; Panels, J. E.; Yan, S. G. Dependence of PEM fuel cell performance on catalyst loading. *J. Power Sources* **2004**, *27*, 162–171.

(29) Mahlon, S.; Gottesfeld, S. High performance catalyzed membranes of ultra-low Pt loading for polymer electrolyte fuel cells. *J. Electrochem. Soc.* **1992**, *139*, L28–30.

(30) Gasteiger, H. A.; Gu, W.; Makharia, T.; Mathias, M. F.; Sompalli, B. Beginning-of life MEA performances: efficiency loss contributions. In *Handbook of fuel cells-fundamentals, technology and applications*, 3; Vielstich, W., Lamm, A., Gasteiger, H. A., Eds.; Wiley: Chichester, U.K., 2003; Chapter 46, p 593.

(31) Edelstein, A. S.; Cammarate, R. C. *Nanomaterials: Synthesis, properties and applications*, 2nd ed.; Institute of Physics: London, 2004; Series in Micro and Nanoscience and Technology, p 433.

(32) Chang, I. S.; Jang, J. K.; Gil, G. C.; Kim, M.; Kim, H. J.; Cho, B. W.; Kim, B. H. Continuous determination of biochemical oxygen demand using microbial fuel cell type biosensor. *Biosens. Bioelectron.* **2004**, *19*, 607–613.

**Table 1. Electrodes Tested in Microbial Fuel Cell (MFC)**

anode electrode	cathode electrode	thickness of Pt (Å)	note
case 1 carbon paper	carbon paper	none	TGPH-120, E-TEK
case 2 Pt-black	carbon paper	1500	electrochemical deposition
case 3 e-beam Pt	carbon paper	1000	e-beam evaporation
case 4 commercial Pt	carbon paper	2500	Pt-black on Vulcan XC-72, E-Tek
case 5 e-beam Pt	carbon paper/ e-beam Pt	1000	e-beam evaporation
case 6 commercial Pt	carbon paper/ commercial Pt	2500	Pt-black on vulcan XC-72, E-Tek

in a mixture solution of 1 mM  $\text{H}_2\text{PtCl}_6$  and 100 mM HCl at room temperature. (2) The other type of electrode was prepared by depositing a 1000 Å Pt layer on the carbon paper using an e-beam evaporator (VE-180, Thermionics Laboratory Inc., U.S.A.) following a manual process provided by the manufacturer.<sup>34</sup> In addition to the two types of electrodes, commercial electrodes (ELSA V2.1 hand-fabricated, single-sided coatings) purchased from E-Tek were examined for comparison.

Since the carbon electrode substrate consists of numerous crossed straight carbon rods, it is difficult to measure the thickness of deposited Pt layers directly. Therefore, we measured the weight of the electrode substrate before and after deposition. Using a Pt density of 21.4 g/cm<sup>3</sup> and the Pt-covered area, the equivalent thickness of Pt layers was calculated as tabulated in Table 1. This method was applied to the electrochemical as well as e-beam depositions. In addition, the thickness of e-beam deposited Pt layers was cross-checked by measuring the thickness of the Pt layer on a monitoring flat wafer that was loaded together with the carbon paper substrates into the e-beam evaporator chamber (Figure 1E).

**E-Beam Evaporation Process.** Evaporation is one of the most frequently used methods for physical deposition. High-energy electron beams directed by a magnetic field locally melt and evaporate target materials. Then, the target vapor is deposited on the desired sample substrates. When this deposition method is used, thin films from several nanometers to 1 μm can be produced with strong adhesion and high surface quality. In this study, we used an e-beam evaporation system that can hold up to a 4-in. wafer. A built-in thin-film crystal (Inficon) was used to monitor the deposition rate and thickness of the films in situ. After venting the evaporator chamber, carbon paper substrates and a crucible containing Pt pellets were loaded into the chamber. When the pressure of the chamber reached about 10<sup>-7</sup> Torr, the high voltage option on the evaporator was activated. The density and the z-ratio of Pt were set at 21.40 g/cm<sup>3</sup> and 0.245, respectively, in the manual mode. An e-beam was directed on the center of the Pt target pellets using an X–Y sweep function. After the Pt was fully melted and outgassed, the emission current was increased to 0.17 A. As soon as the shutter was opened, Pt deposition started and continued until the thickness deposited on the crystal monitor reached 1000 Å.

**Microbial Fuel Cell System.** The microbial fuel cell system used is schematically illustrated in Figure 2. The anode and cathode compartments were separated by a cation exchange membrane (Nafion-112, Dupont, U.S.A.). The anode, external resistor (10 Ω), and cathode were serially connected via platinum wires.<sup>2</sup> In this MFC, the anode compartment was continuously provided with nitrogen gas to maintain anaerobic conditions while the cathode compartment was provided with water-saturated air. The two compartments each contained a sheet of electrode paper (4.0 cm × 1.0 cm). The MFC was electrically loaded with the fixed external resistor (10 Ω). The potential across the resistor was measured by a multimeter (Keithley 2701, Keithley Inc. U.S.A.), which was connected in parallel, and recorded to a personal computer through a data acquisition system<sup>16</sup> controlled with a Labview (National Instrument Inc. U.S.A.) program. The measured potential was converted to an electric current using the following equation:

current (A) = potential (V)/resistance (Ω). We calculated the current density (A/m<sup>2</sup>) using the measured current and the electrode area.

**Characterization of Electrode Surface.** The carbon paper, Pt-black, and e-beam Pt electrodes were imaged using scanning electron microscopy (SEM; e-LiNE, Raith GmbH, Germany) set at 10.0 kV. To cross-check the Pt thickness for e-beam Pt electrodes, a dummy silicon wafer was loaded together with the carbon papers into the e-beam evaporator. The thickness of the Pt layer deposited on the dummy silicon wafer was measured using atomic force microscopy (XE-100, PSIA, Korea).

## Results and Discussion

**Electrode Characterization.** Before installing the fabricated electrodes to an MFC, we first examined their microscopic structures. Two different Pt layer thicknesses (1000 and 1500 Å) were prepared for the Pt-black electrode using the electrochemical deposition method, while a Pt layer of 1000 Å was deposited for the e-beam Pt electrode using the e-beam evaporator. Microscopic views of each electrode were obtained using SEM, as shown in Figure 1. Figure 1A shows a microscopic view of the carbon paper electrode without any Pt depositions. Numerous straight carbon rods cross over each other, layer-by-layer, forming a meshlike structure. When a Pt layer of 1000 Å was electrochemically deposited on the carbon rods, the color of the carbon rods changed from dark gray to shiny gray, as shown in Figure 1B. However, this color change only appeared in several top-end layers of the carbon rods while the carbon rods in the deep layers were not covered with any Pt. This was because the fresh solution in the electrochemical deposition process could not reach the deep layers during the given deposition time. As a result, the overall coverage and uniformity of the Pt layer was very poor. By increasing the amount of deposited Pt, the coverage and uniformity can be improved, as shown in Figure 1C. In this case, the thickness of the Pt layer was measured at 1500 Å. Most of the area of exposed carbon rods was covered with Pt. However, the surface of the deposited surface was rough; that is, there was nonuniform Pt thickness over the electrode area. Figure 1E shows the e-beam Pt-deposited carbon rods. The entire area of the exposed carbon rods was uniformly covered with Pt, although the Pt thickness (1000 Å) was lower than that of the Pt-black electrode of 1500 Å (Figure 1C). Furthermore, the surface was very smooth, indicating that the deposited Pt layer thickness was highly uniform. Figure 1E shows an atomic force microscopy (AFM) image of the Pt layer edge on the dummy silicon wafer that was loaded during the e-beam-deposition process. It was confirmed from the AFM image that the thickness of the e-beam deposited Pt layer was almost 1000 Å. Generally, e-beam deposition provides better coverage on projected surfaces than electrochemical deposition. As a result, given a particular thickness of the Pt layer, e-beam deposition involves less Pt loading than electrochemical deposition. In addition to this advantage, the e-beam deposition also provides strong adhesion between the electrode and the underneath carbon surface. We confirmed that the e-beam electrodes survived 1 h of sonification with little damage while the Pt-black electrodes were easily segregated from the underneath surface by the sonification (data not shown).

**MFC Testing with Pt-Deposited Anode Electrodes.** We investigated the characteristics of electricity generation in MFCs installed with different types of electrodes on the anode compartment: carbon paper electrode (case 1), Pt-black electrode (case 2), e-beam Pt electrode (case 3), and commercial Pt electrode (case 4) (Figure 3). The Pt thickness was 1500 Å for case 2, while it was 1000 Å for case 3. We did not test the Pt-black electrode of 1000 Å since the Pt coverage was poor, as shown in Figure 1B. As shown in Figure 3, for case 1, the current density remained steadily below 0.05 A/m<sup>2</sup> throughout

(33) Diekert, G. The acetogenic bacteria. In *The prokaryotes*, 2nd ed.; Balows, A., Truper, H. G., Dworkin, M., Harder, W., Schleifer, K. H., Eds.; Springer: New York, 1991; pp 517–533.



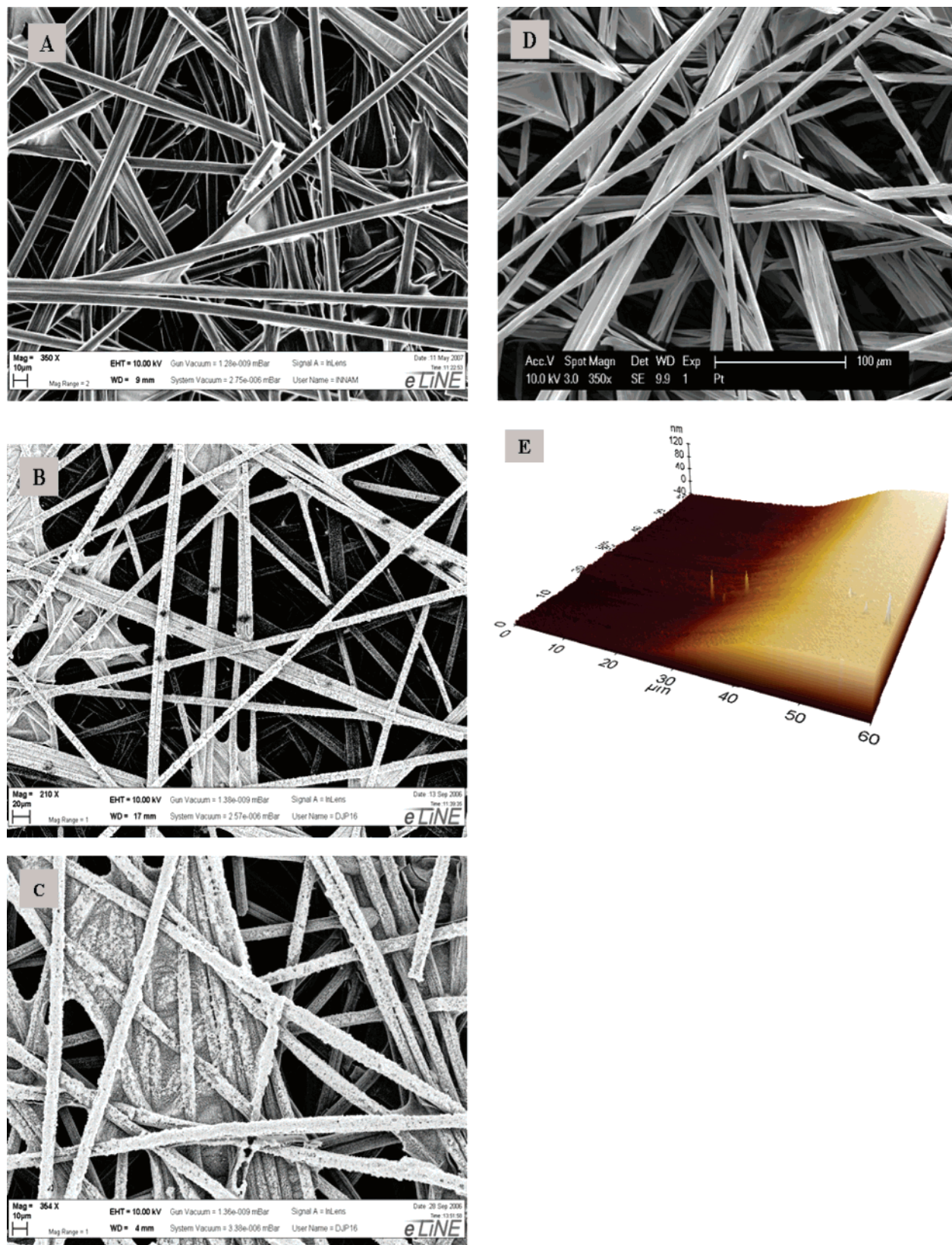


**Figure 1.** SEM photo of carbon paper electrode, Pt-black electrode, and e-beam Pt electrode. Carbon rods on the electrode without Pt deposition (A), Pt-black 1000 Å (B), Pt-black 1500 Å (C), e-beam Pt 1000 Å (D). AFM image of the Pt layer deposited by the e-beam evaporator on a dummy silicon wafer to monitor the deposited Pt thickness (E).

the testing period of 40 h. For case 2, the current density was monotonically increased to  $0.23 \text{ A/m}^2$  in the initial period of about 7 h and remained at a similar level for the rest of the testing period. Case 4 also showed a similar trend. However, it took longer to reach a peak value of  $0.22 \text{ A/m}^2$ . This was due

to different catalytic reactions (in case 4, the Pt as well as the Vulcan XC-72 carbon catalyst on a carbon paper involved catalytic reactions). In the meantime, for case 3 (e-beam Pt electrodes), the current density reached the highest value of  $0.42 \text{ A/m}^2$  among the four cases, which was about 2 times greater

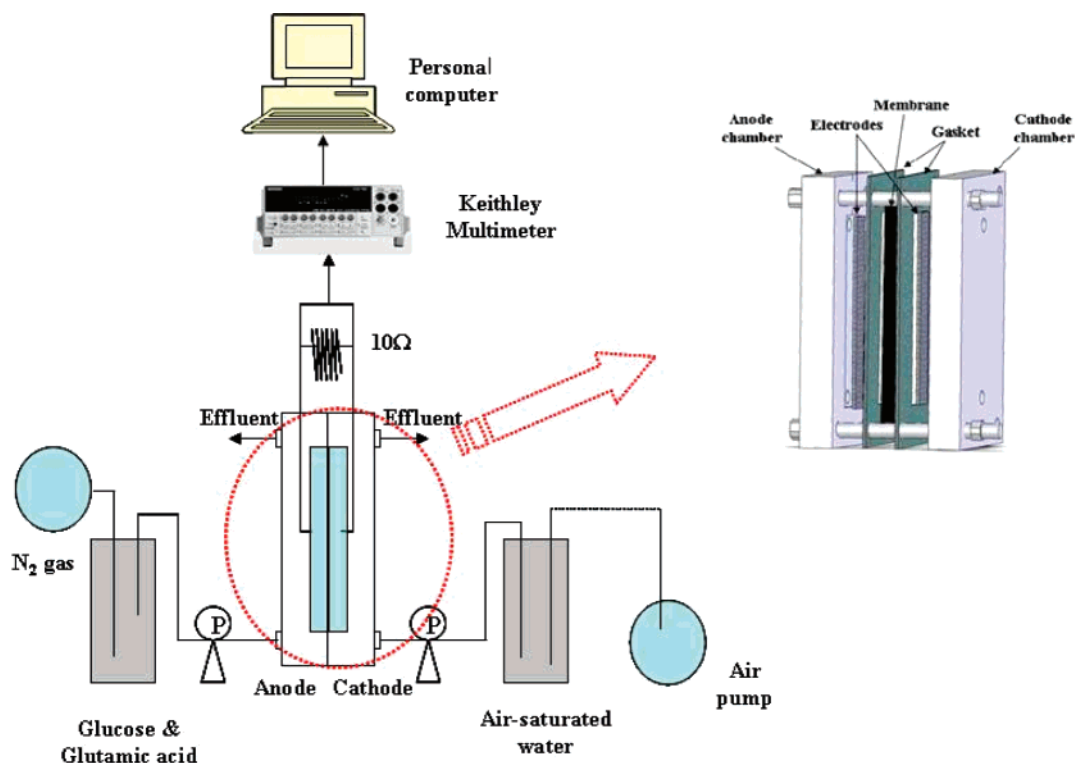


**Figure 2.** Schematic of testing microbial fuel cells. The anode and cathode compartments are separated by a cation exchange membrane. Electrodes are serially connected to a resistance ( $10\ \Omega$ ) using platinum wires and to a multimeter in parallel. The two compartments each contain a sheet of electrodes ( $4.0\text{ cm} \times 1.0\text{ cm}$ ).

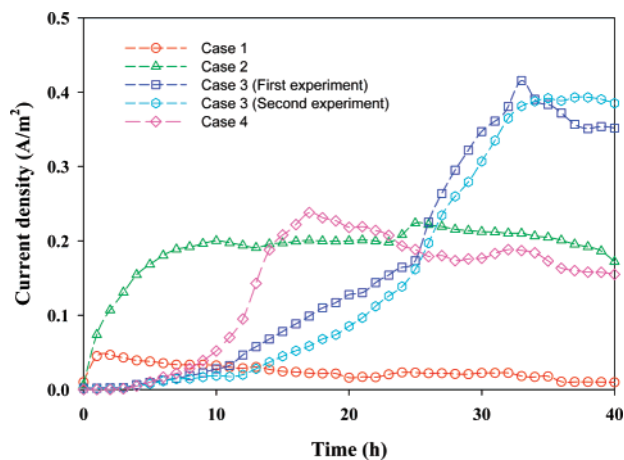


**Figure 3.** Current density when different types of electrodes are installed only on the anode (carbon paper electrode on the cathode in all the cases). Case 1 ( $\circ$ ) is for a carbon paper electrode without Pt; case 2 ( $\Delta$ ) is for a Pt-black electrode ( $1500\ \text{\AA}$ ); case 3 ( $\square$ ,  $\circ$ ) is for an e-beam Pt electrode ( $1000\ \text{\AA}$ ), and case 4 ( $\diamond$ ) is for a commercial Pt electrode ( $2500\ \text{\AA}$ ).

than those of cases 2 and 5 (Pt-black and commercial electrodes, respectively). Recalling that the thickness of Pt for case 3 was only  $1000\ \text{\AA}$ , which was thinner than that for case 2 ( $1500\ \text{\AA}$ ) and case 5 ( $2500\ \text{\AA}$ ), this was a remarkable improvement due mainly to the excellent coverage and uniformity of Pt for the e-beam deposition process as opposed to the electrochemical deposition process.

Another distinct difference between cases 2 and 3 was the initial behavior in the current density. While the current density for case 2 initially increased quickly and flattened out soon afterward, the current density for case 3 increased very slowly for the first 10 h and increased quickly after the 10 h mark. Interestingly, at 24 h, the current density jumped to a peak value. The second run for case 3 shows a similar result. Overall, case

3 showed a delayed response. This delay may be attributed to slow interactions between microorganisms and the Pt catalytic layer. To understand this phenomenon fully, more in-depth studies are required. Despite the delayed response, the total area under the current density curve for case 3 is comparable to that of the curve for case 2 or 4, which means that the e-beam anode electrode using less Pt catalysts produces a total current density comparable to that of case 2 or 4.

Although data are not shown here, we observed that the current density for all the above cases monotonically decreased after hitting the peak values, as Hoster et al. reported and explained; Pt catalytic activities become deteriorated in the fuel cell due to CO poisoning during fuel oxidation.<sup>24</sup>

**MFC Testing with Pt-Deposited Anode and Cathode Electrodes.** The results in the previous section show that Pt on the anode electrode significantly improves the current density. This section investigates the effects of Pt on MFC performance when Pt is deposited on the cathode as well as anode electrodes. Since the current density in case 1 was substantially low and the current density in case 2 was similar to that of case 4, our scope was more focused on the configurations of cases 3 and 4. First, we installed the e-beam Pt electrodes in both the cathode and anode compartments and ran the MFC. However, the current density was similar to the current density in case 3 (data not shown) without any significant improvement. The Pt layer on the cathode did not seem to have any noticeable influence on the current density. However, when the Pt electrode was installed on the cathode after a certain number of hours running with a carbon electrode on the cathode, we noticed a significant change in the current density, as shown in Figure 4. Case 5 was where the carbon paper on the cathode was replaced with an e-beam Pt electrode after 45 h of running the MFC under the conditions used in case 3. After the cathode electrode replacement, the current density immediately jumped to a higher level than before, and it continued to rise. The maximum current density measured  $0.50\text{ A/m}^2$ , which was higher than the first peak ( $0.42$



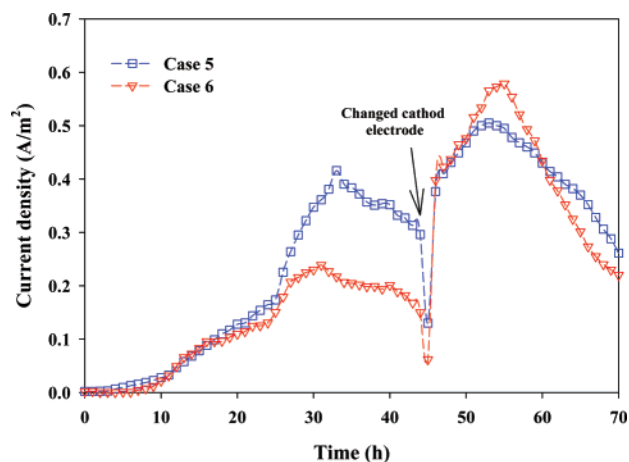


**Figure 4.** Current density for cases 5 ( $\square$ ) and 6 ( $\nabla$ ). In case 5, the e-beam Pt electrode is installed on the anode while the carbon paper electrode is installed on the cathode prior to reaching 45 h. In case 6, the commercial Pt electrode is installed on the anode while the carbon paper electrode is installed on the cathode prior to reaching 45 h. At 45 h, the carbon paper on the cathode is replaced with an e-beam Pt electrode (case 5) and a commercial Pt electrode (case 6).

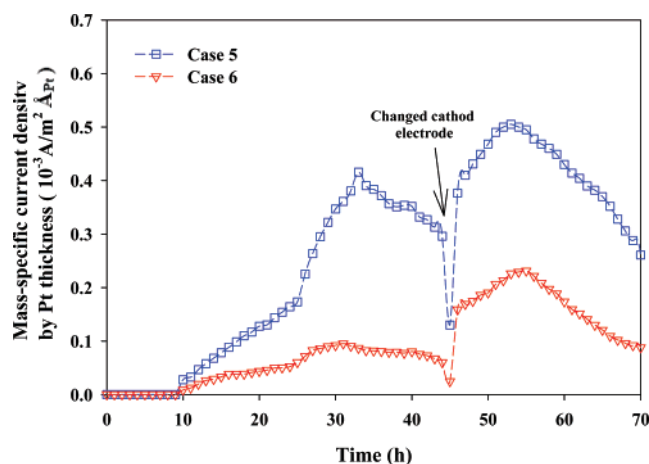


**Figure 5.** The mass-specific current density that represents the current density per unit Pt thickness. This figure was produced after dividing the current density in Figure 4 by the corresponding Pt thickness.

$\text{A/m}^2$ ). Similarly, the cathode replacement was made on case 4; the carbon paper on the cathode was replaced with a commercial Pt electrode (E-Tek electrode; named case 6) after 45 h of running under the same conditions as case 4. After the cathode replacement, the current density also jumped and reached a maximum value of  $0.60 \text{ A/m}^2$ . For the two cases (cases 5 and 6), the replacement of the carbon electrode on the cathode with the e-beam Pt electrode led to an increase in the current density, thus generating the second peaks, which were higher than the first peaks. In the mean time, it is known that replacing the electrodes in the middle of a run causes a current increase. To check this, we simply replaced the carbon cathode with a new normal carbon electrode (no Pt) after 45 h of running. Similarly, we observed a jump in the current density, but its magnitude was about 40% lower than that for the e-beam Pt electrode case.

The second peak in case 6 ( $0.60 \text{ A/m}^2$ ) was higher than the one in case 5 ( $0.50 \text{ A/m}^2$ ). However, considering the thickness of Pt on the electrodes, the e-beam electrodes were more effective than the commercial Pt electrodes. Figure 5 shows the mass-specific current density for cases 5 and 6, which was reproduced by dividing the current density by the corresponding Pt thickness. In case 5, the mass-specific current density was higher than the one in case 6 during the entire range of the

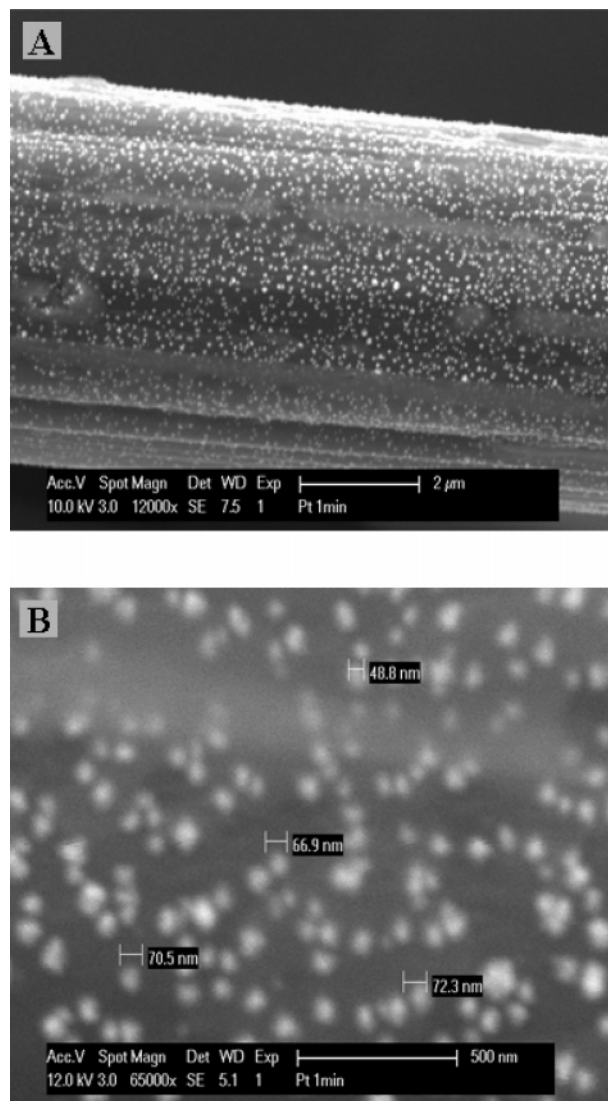


**Figure 6.** SEM photos of Pt nanoparticle electrodes fabricated by the e-beam evaporator. (A) Nanoparticles on carbon paper and (B) a magnified view of the nanoparticles.

testing period. The peak value for case 5 was 2.5 times higher than the one for case 6. This result suggests that e-beam electrodes are highly effective and cost-effective in current generation regardless of whether the Pt electrodes are installed on the anode only or on both the anode and the cathode. It is speculated that this is due mainly to the excellent coverage and strong adhesion of the e-beam Pt layer on the underneath layer.

**Maximum Power Density.** The current density can be readily interpreted in relation to the power density. In this work, we achieved a maximum power density of  $2500 \text{ mW/m}^2$  using e-beam Pt electrodes on both an anode and a cathode (case 5). This value was higher than the previous results in the literature: for example,  $1030 \text{ mW/m}^2$  with Pt ( $1500 \text{ \AA}$ )/nafion on a cathode in Jong et al.,<sup>35</sup>  $560 \text{ mW/m}^2$  with Pt ( $1500 \text{ \AA}$ )/nafion on a cathode in Moon et al.,<sup>36</sup> and  $480 \text{ mW/m}^2$  with Pt ( $2500 \text{ \AA}$ )/PTFE and  $369 \text{ mW/m}^2$  with Pt ( $2500 \text{ \AA}$ )/CoTMPP on a cathode in Cheng et al.<sup>7</sup> These results indicate the potential of e-beam Pt electrodes that are practically used for MFCs.

(34) VE-series vacuum coating systems general instruction manual, Thermionics laboratory Inc., p 10–17, 2007.

(35) Jong, B. C.; Kim, B. H.; Chang, I. S.; Liew, P. W. W.; Choo, Y. F.; Kang, G. S. Enrichment, performance, and microbial diversity of a thermophilic mediatorless microbial fuel cell. *Environ. Sci. Technol.* **2006**, *40*, 6449–6454.

The ease of the setting change in e-beam deposition provided an additional advantage, allowing us to deposit Pt in the form of nanoparticles, as shown in Figure 6. It was expected that the Pt nanoparticles would substantially augment catalytic reactions due to extremely high surface areas. In addition, e-beam deposition allows us to deposit Pt alloys as well, such as Pt/Ru, which is known to enhance the stability of current density.<sup>23,24</sup> These topics are currently under investigation and will be published in different articles in the near future.

### Conclusions

Electricity generation in MFCs was investigated by implementing e-beam deposited Pt electrodes into an anode and a cathode. Pt is known to act as an excellent catalyst in fuel cell reactions. Due to its high cost, however, Pt loading without any performance compromise has long been a primary concern. In this study, to minimize the loading of Pt, a Pt layer of 1000 Å in thickness was deposited on a carbon paper anode and cathode using an e-beam evaporator. Before installing these electrodes into MFCs, we characterized their microscopic structures along with Pt-black electrodes (electrochemically deposited) using SEM and AFM, confirming greater coverage of the e-beam Pt layer and stronger adhesion than the electrochemically deposited

Pt-black electrodes. Then, the current density was examined after installing the e-beam electrodes only on the anode in MFC (carbon paper electrode on the cathode). Also, other types of electrodes such as Pt-black electrodes, commercial Pt electrode (E-Tek), and carbon electrodes were examined and compared. Among them, the e-beam Pt electrode showed a highest peak value in the current density, which was about 2 times higher than that of the Pt-black electrode or E-Tek commercial Pt electrode. In addition, it was shown that replacement of the carbon cathode electrode with an e-beam electrode after 45 h of MFC running generated an immediate increase in the current density, reaching a second peak. A similar result was obtained with a commercial Pt electrode replacement. However, considering that the e-beam electrode had the least thick Pt layer among the tested electrode types, the e-beam electrode was the most effective in terms of mass-specific current density. These results suggest the potential of e-beam deposited Pt electrodes in improving MFC efficiency with minimal loading of Pt.

**Acknowledgment.** This work was supported by the Mascaro Sustainability Initiative (MSI) at the University of Pittsburgh. The authors would like to thank James C. Brucker at the wastewater treatment plant of the Franklin Township Municipal Sanitation Authority in Pittsburgh.

EF070160X

---

(36) Moon, H.; Chang, I. S.; Kim, B. H. Continuous electricity production from artificial wastewater using a mediator-less microbial fuel cell. *Bioresour. Technol.* **2006**, 97 (4), 621–627.